

High Voltage and High Capacity Characteristics of $\text{LiNi}_{1/3}\text{Co}_{1/3}\text{Mn}_{1/3}\text{O}_2$ Cathode for Lithium Battery Applications

P.Periasamy¹, N.Kalaiselvi^{1,*}, H.S.-Kim²

¹ Electrochemical Power Systems Division, Central Electrochemical Research Institute[CECRI], Karaikudi, India

² Advanced Materials for Applied Research Laboratory, KERI, Changwon, South Korea

*E-mail: kalakanth2@yahoo.com

Received: 14 June 2007 / Accepted: 1 August 2007 / Published: 1 September 2007

Possibility of synthesizing $\text{LiNi}_{1/3}\text{Co}_{1/3}\text{Mn}_{1/3}\text{O}_2$ cathode via., soft chemistry based Gelatin Assisted Combustion [GAC] approach has been examined through the present study. GAC method with a calcination temperature as high as 750°C for a period of 24h. was found to be essential to prepare $\text{LiNi}_{1/3}\text{Co}_{1/3}\text{Mn}_{1/3}\text{O}_2$ powders with good hexagonal ordering and better cycling performance. The intensity ratio of (003) and (104) bragg peaks is greater than unity, which is an indication for the absence of cation mixing. The observed CV peaks confirm the presence of Ni, Co and Mn ions in their +3 oxidation state. A maximum discharge capacity of $\sim 180\text{mAh/g}$ has been exhibited by the synthesized $\text{LiNi}_{1/3}\text{Co}_{1/3}\text{Mn}_{1/3}\text{O}_2$ cathode, when charged up to 4.6V. Hence, it is demonstrated that the $\text{LiNi}_{1/3}\text{Co}_{1/3}\text{Mn}_{1/3}\text{O}_2$ cathode synthesized through the present study could be exploited both as a high voltage and high capacity cathode material for use in rechargeable lithium battery applications.

Keywords: Gelatin Assisted Combustion [GAC] method, $\text{LiNi}_{1/3}\text{Co}_{1/3}\text{Mn}_{1/3}\text{O}_2$ cathode, specific capacity, lithium batteries

1. INTRODUCTION

Apart from the present application of lithium-ion batteries as power sources for portable electronics that includes 3C applications, they are being considered as the promising candidates for use in EVs in future. Driven away due to the high cost and toxic nature of LiCoO_2 and LiNiO_2 cathodes, recent studies have a special focus on Li-Mn-O based systems as alternative cathode materials. In contrast to LiMn_2O_4 , trivalent LiMnO_2 possesses a high theoretical capacity of 285mAh/g , which is twice that of LiMn_2O_4 [1,2], and is reported to exhibit better cycleability even between 2.0 and 4.5V vs. Li^+/Li . In orthorhombic LiMnO_2 , oxygen ions are arranged in nearly cubic close packing, and the octahedral interstices are occupied by Li and Mn, forming corrugated layers

[3]. Due to the presence of high spin Mn^{3+} ($t_{2g}^2e_g^1$) on the O_h sites, the local symmetry around Mn^{3+} is distorted due to Jahn-teller distortion. So, the Mn sub lattice can be viewed as a folded triangular lattice and the fold angle being 111° . i.e., each triangle is distorted to isosceles with one edge of $2.806^\circ A$ and other two of $3.09^\circ A$ [4].

Despite the merits of $LiMnO_2$ cathode such as low material cost, high energy density, high working voltage and acceptable environmental characteristics etc., requirement of prolonged high temperature heating and the consequences of the same to cause severe coarsening of the cathode powder that results in the volatilization of lithium compounds [5] are the major issues against the global acceptance of $LiMnO_2$ in its native form. In addition, it is reported that the transformation from orthorhombic structure to spinel like structure becomes easier and faster with the increase in the degree of stacking faults [6-9]. Therefore, towards the preparation of orthorhombic $LiMnO_2$ powders with a rock salt structure, precise control of oxygen content in the heating atmosphere is to be monitored strictly.

Nevertheless, $LiMnO_2$ may be stabilized as a layered structure by the partial substitution of metals, as dopants, provided suitable synthesis methods are adopted. Because, the crystal stability during intercalation and de-intercalation of lithium could be enhanced by the partial substitution of suitable dopants. In addition, the partial substitution is found effective not only for the stabilization of the layered structure, but also for the generation of higher red ox potentials, in certain cases[10]. Towards this direction, Cr, Ti, Mg, Ni, Al and V have been incorporated as dopants in to $LiMnO_2$ matrix to display good electrochemical performance [11-12]. In other words, partially substituted Cr^{3+} and Al^{3+} cations are reported to reduce the tendency of the layered structure converting to the more stable spinel via. prevention of cation redistribution. Also, the dopants are believed to dilute the Jahn-Teller distortion by partial substitution for the Mn ions [13]. Because, substitution of Co is reported to exhibit 50% increase in the amount of lithium that can be removed and reinserted in to the oxide frame work, thereby improving the capacity retention. Also, it is reported that the rate of conversion of o- $LiMnO_2$ in to spinel $LiMn_2O_4$ is controlled significantly by the presence of cobalt dopant [14].

So, it is with this background that the present study has been designed to synthesise and characterize the simultaneously substituted Co and Ni cations in the $LiMnO_2$ matrix with a view to understand the synergistic effect of both the dopant cations towards the enhancement of electrochemical properties of $LiNi_{1/3}Co_{1/3}Mn_{1/3}O_2$. In this connection, a novel and a simple Gelatin Assisted Combustion [GAC] method [15] has been deployed to explore the possibility of synthesizing orthorhombic $LiMnO_2$ substituted simultaneously with equal amounts of Co and Ni to arrive at single phasic $LiNi_{1/3}Co_{1/3}Mn_{1/3}O_2$. The advantages and the significance of GAC method in synthesizing battery active Li-M-O type of cathode materials has already been mentioned elsewhere [15].

In short, the present study enumerates the advantages of partial substitution of Co and Ni on $LiMnO_2$ matrix in enhancing the electrochemical characteristics of the resultant $LiNi_{1/3}Co_{1/3}Mn_{1/3}O_2$ cathode material. Also, the study demonstrates the possibility of synthesizing $LiNi_{1/3}Co_{1/3}Mn_{1/3}O_2$ cathode via., a one-pot GAC method in its pure and electrochemically active form, the prime factor required for global acceptance.

2. EXPERIMENTAL PART

Stoichiometric amounts of nitrates of lithium, cobalt, nickel and manganese (1:1:1 wt%) were dissolved in double distilled water to get a clear solution. To this solution was added a well stirred solution of gelatin in water and the resultant homogenous solution was heated initially at 90-100°C for 1 h. to obtain a viscous solution. The viscous solution thus obtained was dried at 120°C for 12 h. and subjected further to different calcination temperatures such as 300°C, 600°C and 750°C individually. Heat treatment at various temperatures was carried out mainly to understand the effect of calcination temperature upon synthesizing phase pure compound and to identify the optimum temperature required to synthesize better performing $\text{LiNi}_{1/3}\text{Co}_{1/3}\text{Mn}_{1/3}\text{O}_2$ compound through GAC method. Based on the results of optimization study, calcination temperature not less than 750°C was found to be highly essential to obtain phase pure products of $\text{LiNi}_{1/3}\text{Co}_{1/3}\text{Mn}_{1/3}\text{O}_2$ cathode. Consequently, the 750°C heat treated precursors were examined further with furnace heating for various dwelling times such as 3h., 6h., 12h. and 24h. individually, with a view to understand the effect of dwelling time upon calcination in modifying the physical as well as electrochemical properties of the synthesized $\text{LiNi}_{1/3}\text{Co}_{1/3}\text{Mn}_{1/3}\text{O}_2$ powder. The ultra fine powders obtained at the end of the final calcination process has been collected and subjected to the following characterization studies.

The phase purity of the product was verified using a Philips X-ray diffractometer. XRD patterns were recorded using nickel-filtered $\text{Cu-K}\alpha$ radiation at room temperature in the 2θ ranges 10-90 at a scan rate of 0.02°s^{-1} . Surface morphology of the particles was examined using SEM images obtained from Jeol S-3000 H Scanning Electron microscope. Cyclic voltammetry, A.C. impedance and Charge discharge studies were carried out with the crimp sealed 2016 coin cells. Lithium metal was used as the anode and 1M LiPF_6 in 1:1 v/v ethylene carbonate (EC): dimethyl carbonate (DMC) as electrolyte. The cathode was prepared by mixing 85% active material with 5% super-P carbon and 10% poly (vinylidene fluoride) (PVdF) binder in N-methyl-2-pyrrolidone (NMP), which was coated on an aluminium foil and dried at 120°C for 3h in an oven. The resulting $\text{LiNi}_{1/3}\text{Co}_{1/3}\text{Mn}_{1/3}\text{O}_2$ coating on aluminium foil was roll pressed and the electrode was punched out in the required dimension with a punching machine. 2016 coin cells were assembled in an organ filled glove box and cycled at different cut-off voltages using Toyo multi channel battery cycle life tester. Electrochemical Impedance Measurements and CV studies were performed on a TOSCAT Spectrophotometer.

3. RESULTS AND DISCUSSION

3.1. Physical characterization studies

3.1.1. XRD studies

X-ray diffraction analysis was carried out for the GAC [Gelatin Assisted Combustion] synthesized $\text{LiNi}_{1/3}\text{Co}_{1/3}\text{Mn}_{1/3}\text{O}_2$ products synthesized at various calcination temperatures to monitor the evolution of compound formation, development and attainment of high degree of phase purity and crystallinity. Basically, the $\text{LiNi}_{1/3}\text{Co}_{1/3}\text{Mn}_{1/3}\text{O}_2$ powders obtained from high calcinations

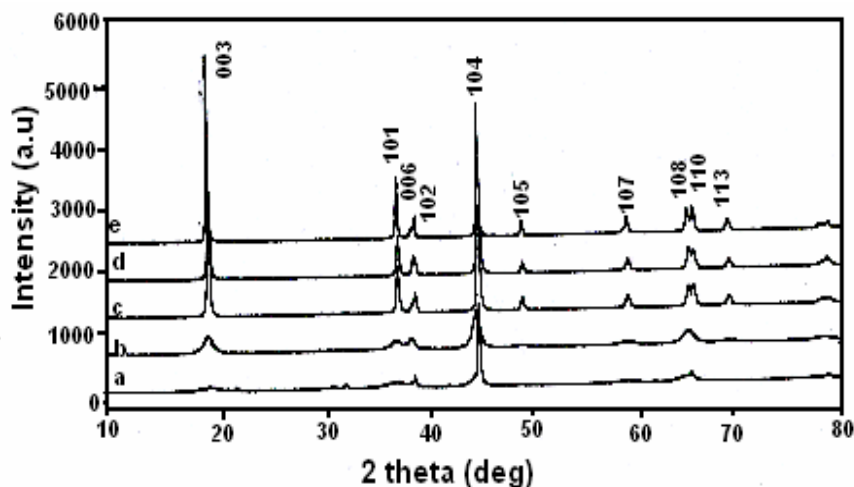


Figure 1. PXRD pattern observed for $\text{LiNi}_{1/3}\text{Co}_{1/3}\text{Mn}_{1/3}\text{O}_2$ cathode prepared at a) 300°C (3h.); b) 600°C (3h.); c) 750°C (3h.); d) 750°C (12h.) and 750°C (24h.)

temperatures such as 600 and 750°C are black in color and are stable towards exposure to air and moisture.

The XRD pattern of high temperature treated $\text{LiNi}_{1/3}\text{Co}_{1/3}\text{Mn}_{1/3}\text{O}_2$ powders exhibited well defined peaks corresponding to the $\alpha\text{-NaFeO}_2$ structure with $R3m$ space group. Presence of undesirable peaks due to impurities are not seen in the Bragg pattern. So, the transition metal atoms, viz., Ni, Mn and Co are expected to distribute randomly on 3b sites, lithium on 3a sites and the oxygen atoms on 6c sites. It can be seen from Fig.1 that a completely amorphous structure has been obtained for the precursor powder heated at 300°C (Fig.1a). On the other hand, XRD pattern of the sample heat treated at 600°C shows the presence of characteristic bragg peaks (Fig.1b), indicating the formation of $\text{LiNi}_{1/3}\text{Co}_{1/3}\text{Mn}_{1/3}\text{O}_2$ compound at this temperature. Further, it is understood that even though the compound formation had taken place at 600°C , the process of crystallinity seems to be incomplete, as inferred from the minimal intensity observed for the entire set of peaks recorded for the sample prepared at 600°C . So, post calcination at 750°C was felt to be essential [16] and hence heating the sample at 750°C for different time duration (3h., 12h. & 24h.) was carried out with a view to understand whether extended dwelling period at 750°C would impart any favorable physical and/or electrochemical performance characteristics of $\text{LiNi}_{1/3}\text{Co}_{1/3}\text{Mn}_{1/3}\text{O}_2$ samples. The bragg pattern corresponding to such powders are depicted in Figs. 1c-e.

It is quite interesting to note that the intensity ratio of (003) and (104) peaks is greater than unity, i.e. $I_{(003)}/I_{(104)} > 1$ and clear doublets such as (006), (102) and (108), (110) have been observed, which corresponds to the absence of cation mixing, encountered normally with the layered structure. Generally, the presence of independently formed (101) along with (006) and (102) doublet possessing more or less similar peak pattern is assigned to the homogeneity and phase purity of layered LiNiO_2 related compounds[17] and such a bragg pattern has been produced by $\text{LiNi}_{1/3}\text{Co}_{1/3}\text{Mn}_{1/3}\text{O}_2$ synthesised at 750°C (3h.). Rest of the compounds synthesised at relatively lower temperatures, viz.,

300 and 600°C (Figs.1a&b) have exhibited either two or three distinct peaks with asymmetrical peak pattern and with lesser visibility. As a result, it is deduced from XRD that a temperature of 750°C for a minimum period of 3h. is unavoidably essential to synthesise $\text{LiNi}_{1/3}\text{Co}_{1/3}\text{Mn}_{1/3}\text{O}_2$ with homogeneity and purity. On the other hand, the compound heated at 750°C for longer duration such as 12h. and 24h. exhibited distinctly spaced doublets like (108),(110) and (106), (112) along with the presence of highly intense singlet peaks (Figs.1d&e). Based on this observation, it is deduced that high calcination treatment at 750°C for 24h. is reasonably essential to obtain $\text{LiNi}_{1/3}\text{Co}_{1/3}\text{Mn}_{1/3}\text{O}_2$ of phase pure and better crystalline nature.

The lattice parameter values viz., $a = 2.82$ and $c = 14.10$ Å respectively are in accordance with the reported values [18]. Also, the calculated c/a ratio (Table 1) strongly favors the exclusion of cation-mixing, as the same is greater than 4.91. Variation of lattice parameters such as a , c , c/a , $I_{(003)} / I_{(104)}$ and unit cell volume of the $\text{LiNi}_{1/3}\text{Co}_{1/3}\text{Mn}_{1/3}\text{O}_2$ samples with respect to variation in heating times are summarized in Table1 along with R-factor details.

Table 1. Variation of different lattice parameters of $\text{LiNi}_{1/3}\text{Co}_{1/3}\text{Mn}_{1/3}\text{O}_2$ compound as a function of calcinations temperature

Calcination Temperature	a (Å)	c (Å)	c/a ratio	$I_{(003)} / I_{(104)}$	R factor $[I_{006}+I_{102} / I_{101}]$	Unit cell volume (Å ³)
600°C (3h.)	2.879	14.231	4.943	0.750	--	102.031
750°C (3h.)	2.870	14.148	4.946	1.085	0.75	100.803
750°C (12h.)	2.854	14.153	4.959	1.342	0.71	100.658
750°C (24h.)	2.877	14.059	4.967	1.347	0.60	99.879

Reimers et. al. [19] reported that the R-factor, which is defined as the ratio of intensities of the characteristic hexagonal doublet peaks viz., (006) and (102) to (101) $[I_{(006)} + I_{(102)} / I_{(101)}]$ is an indicator of hexagonal ordering. From Table1, it is obvious that the R- factor calculated for the $\text{LiNi}_{1/3}\text{Co}_{1/3}\text{Mn}_{1/3}\text{O}_2$ sample heated at 750°C with increasing dwelling time is found to decrease linearly. The lower value of 0.60 is obtained with the 750°C /24h. heat-treated sample, which is an indication for good hexagonal ordering and better cycling performance. Thus, it is concluded that from R-values that a dwelling time of 24h. at 750°C is needed to prepare $\text{LiNi}_{1/3}\text{Co}_{1/3}\text{Mn}_{1/3}\text{O}_2$ powders with good physical as well as electrochemical properties. Further, all the calculated lattice parameter values and unit cell volume are found to have closer agreement with the reported values [20].

3.1.2. SEM studies

SEM image of $\text{LiNi}_{1/3}\text{Co}_{1/3}\text{Mn}_{1/3}\text{O}_2$ sample heated at 750°C captured under a magnification of X 10K is displayed in Fig.2. The formation of mono dispersed spherical grains with clearly seen crystal boundaries are evident from the SEM picture. The process of agglomeration that is expected normally during high temperature calcinations is found to be absent, as the present study accounts to the possibility of synthesizing $\text{LiNi}_{1/3}\text{Co}_{1/3}\text{Mn}_{1/3}\text{O}_2$ with the preferred morphology of reduced grain size in the range of 1µm. This is because, the possible agglomeration of particles has already been

controlled in the earlier stages of furnace heating of the precursor (at 120, 300 and 600°C) by way of slow heating of the homogenous solution/sintered powder. Also the particles obtained after 300°C were subjected to grinding process to get further preferred orientation and the uniform distribution of size reduced particles. The ultimate grain growth controlled particles of uniformly distributed pattern were found to maintain the same even at the high calcination temperature of 750°C (Fig.2), which is the interesting behavior and the beneficial effect due to the adoption of specific heat treatments. Also, the usage of gelatin as combustible fuel is expected to impart some preferred morphological characteristics, thereby leading /promoting the formation of $\text{LiNi}_{1/3}\text{Co}_{1/3}\text{Mn}_{1/3}\text{O}_2$ ultimately, with particulate appearance containing definite grain boundaries. Hence, it is understood that the inclusion of select category combustible fuels as additives in the normal combustion synthesis method along with the process of intermittent grinding and slow rate of heating may have better influence over the physical characteristics not only on the title compound, but also over a wide variety of synthesized compounds, irrespective of the type and nature of the same.



Figure 2. SEM image captured for $\text{LiNi}_{1/3}\text{Co}_{1/3}\text{Mn}_{1/3}\text{O}_2$ cathode synthesized at 750°C (24h.)

3.2. Electrochemical characterisation studies

3.2.1. Cyclic voltametry

Figs.3(a) and (b) show the cyclic voltamogram of $\text{LiNi}_{1/3}\text{Co}_{1/3}\text{Mn}_{1/3}\text{O}_2$ electrode that has been fabricated using the powders synthesized at 750°C for 24h. deployed in 2016 coin cells assembled with Li metal and 1M LiPF_6 in EC:DEC (1:1) electrolyte recorded at 200 $\mu\text{V}/\text{sec}$. and 100 $\mu\text{V}/\text{sec}$. scan rates respectively. In other words, the electrochemical performance of $\text{LiNi}_{1/3}\text{Co}_{1/3}\text{Mn}_{1/3}\text{O}_2$ cathode was studied using cyclic voltametry in the potential range from 3.0 to 4.2V and 4.8V vs. Li/Li^+ wherein Li metal anode has been used both as the reference and counter electrodes. Fig.2a shows the presence of an anodic peak that corresponds to the de-intercalation of Li^+ at 4.0V in a broad potential range. Similarly, it is obvious from Fig.3a that a relatively equal amount of lithium is extracted, as implied by

the cathodic peak at 3.4V. Further, it is demonstrated from CV studies that the first cycle CV pattern differs from the one recorded for the second cycle in the voltage range 3.0~4.2V, wherein oxidation-reduction reaction occurs normally. This is attributed to the possible irreversible loss of capacity at the first cycle [21] and the larger de intercalation currents seen in the cyclic voltammogram agree with the first cycle capacity values [22].

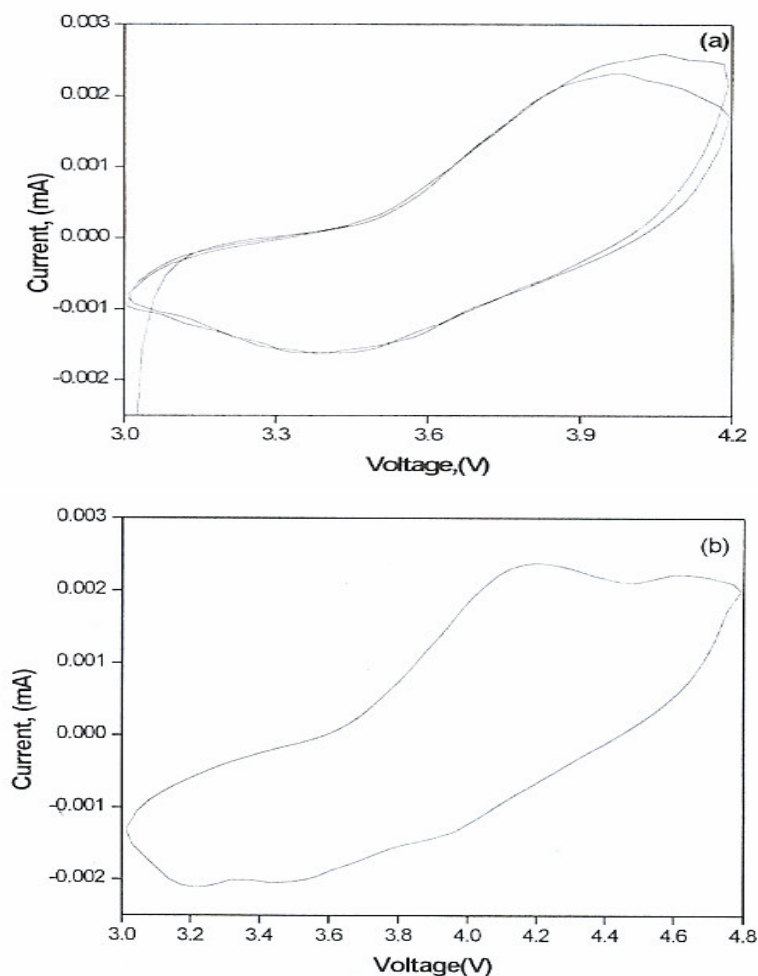


Figure 3. Cyclic voltammogram of $\text{LiNi}_{1/3}\text{Co}_{1/3}\text{Mn}_{1/3}\text{O}_2$ cathode synthesized at 750°C (24h.) against Li metal along with 1M LiPF_6 in 1:1 v/v EC:DEC at $200\mu\text{V}/\text{sec}$. and b) $100\mu\text{V}/\text{sec}$. scan rate

The cyclic voltammogram of $\text{LiNi}_{1/3}\text{Co}_{1/3}\text{Mn}_{1/3}\text{O}_2$ systems (Fig.3b) scanned at $100\mu\text{V}/\text{sec}$. showed a broad oxidation peak potential at 4.1V with a prominent shoulder at 4.0V corresponding to the red ox behavior of Co^{3+} to Co^{4+} [23]. Similarly, red ox peaks observed at 4.6 and 3.6V are attributable to the oxidation of Ni^{3+} to Ni^{4+} and the peak at the 3.2V to that of Mn^{3+} to Mn^{4+} . These results are in good agreement with those of Lu et al [24], thus illustrates the reversibility of the synthesized $\text{LiNi}_{1/3}\text{Co}_{1/3}\text{Mn}_{1/3}\text{O}_2$ material upon de-intercalation and intercalation of lithium-ions over the potential range of 3.0-4.8V versus Li/Li^+ reference electrode.

3.2.2 Impedance studies

Generally, electrochemical impedance studies are carried out to have better understanding of certain aspects of a lithium cell such as failure mechanism [25], self discharge [26], lithium cycling efficiency [27], interfacial phenomenon between electrode and electrolyte [28] and lithium cation diffusion in the electrode and the electrolyte [29]. Among these, the cathode electrodes are normally be given least attention, because problems related to the lithium anode are the main concern for commercialization of rechargeable lithium batteries. But, with the progress in lithium and lithium-ion battery technology, problems related to cathodes are one of the major factors reported to affect the performance of a lithium battery via., unacceptable capacity fade and a huge drop in working cell voltage during discharge. So, electrochemical impedance measurements were recorded for both in the as assembled and in the fully charged states of the $\text{LiNi}_{1/3}\text{Co}_{1/3}\text{Mn}_{1/3}\text{O}_2$ cathodes deployed in 2016 coin cells against lithium metal.

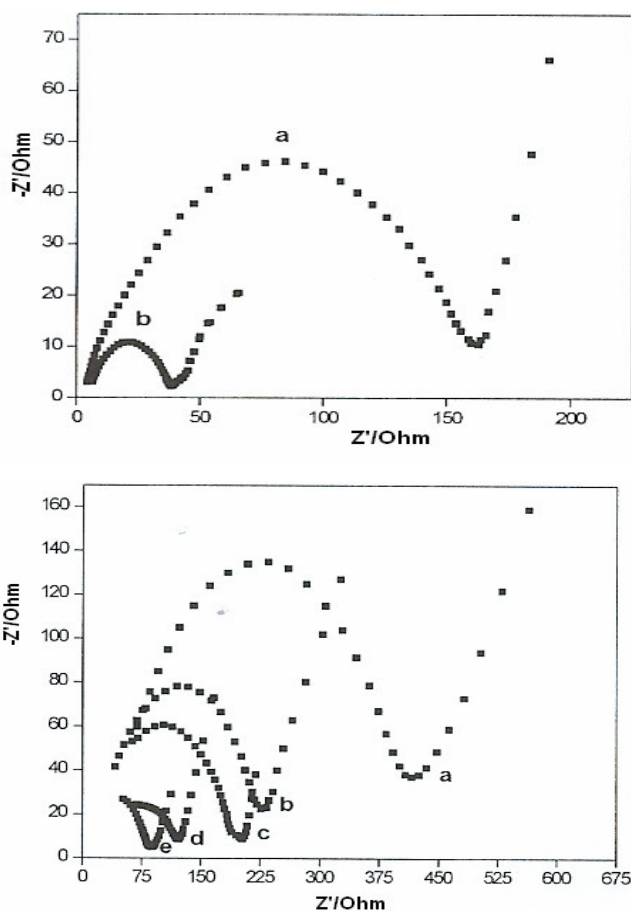


Figure 4. Nyquist plots of $\text{Li}/\text{LiNi}_{1/3}\text{Co}_{1/3}\text{Mn}_{1/3}\text{O}_2$ cells at various state-of-charge, viz., 5% : b)25%; c) 50% ; d)75% and e)100% SOC

Figs.4a&4b shows the Nyquist plots of as assembled and SOC $\text{Li}/\text{LiNi}_{1/3}\text{Co}_{1/3}\text{Mn}_{1/3}\text{O}_2$ cells respectively. Comparison between the nyquist plots of a freshly assembled $\text{Li}/\text{LiNi}_{1/3}\text{Co}_{1/3}\text{Mn}_{1/3}\text{O}_2$

system and the one recorded for the first Li de-intercalation and intercalation cycle are shown in Fig.4a. The high frequency region semi circle in the spectrum of the fresh electrode is much higher than in the spectrum of the cycled electrode [30], an indication for the unavoidable initial irreversible capacity loss behavior of the same upon charge- discharge cycling process.

The impedance spectra of Li/ LiNi_{1/3}Co_{1/3}Mn_{1/3}O₂ cells in the Nyquist plot at various state-of-charge [SOC] values such as 0%, 25%, 50%, 75% and 100% are shown in Fig.4b. A semi circle in the high frequency region and a spike in the low frequency region were characterized by the individually recorded impedance spectrum. Generally, the presence of a semi-circle is attributed to the presence of passive film on the oxide surface [31]. Similarly, the low frequency spike which is an arc of an incomplete semi-circle, is attributed to the charge-transfer resistance of the electrochemical reaction. It can be seen from Fig.4b that the charge transfer resistance is decreased linearly with the increasing charging voltage, which is an indication that the LiNi_{1/3}Co_{1/3}Mn_{1/3}O₂ cathode becomes more conductive at the higher state-of-charge. In other words, the LiNi_{1/3}Co_{1/3}Mn_{1/3}O₂ material has exhibited the lowest R_{ct} values (85 Ohms) in the highly charged state [SOC-100%], which is in favor of the fact that at high charging voltages, the LiNi_{1/3}Co_{1/3}Mn_{1/3}O₂ material turns out to be a good conductor. This may also be attributed to the high drain capability of the system [32], desired for high power lithium battery applications. Hence, it is inferred that a high charging voltage of 4.6V would be advantageous to realize the maximum possible specific capacity as far as LiNi_{1/3}Co_{1/3}Mn_{1/3}O₂ cathodes are concerned.

3.2.3. Charge-Discharge Studies

Variations in the discharge specific capacity (Q_{dc}) with respect to different cut-off voltage as a function of varying furnace heating times, say 3, 12 and 24h. for the compound LiNi_{1/3}Co_{1/3}Mn_{1/3}O₂ are shown in Figs.5a-c. The 20th cycle charge-discharge capacity (Q_{dc20}) values of the sample prepared at 750°C for 12h. was measured as 112.79, 136.14 and 154.14mAh/g with an irreversible capacity of 2.59, 4.28 and 6.64mAh/g as a function of varying cut-off voltages such as 4.2, 4.4 and 4.6V. Such an observation is mainly attributed to the lack of hexagonal ordering that includes the lack of ordering in lithium ion and transition metal ion sites and lower crystallinity [31]. Generally, due to the formation of undesirable oxides, high temperature and longer heating times are required to form a well ordered LiNi_{1/3}Co_{1/3}Mn_{1/3}O₂ phase. Thus, the samples prepared at 750°C for 3 and 12h. that show a reasonable specific capacity (130-145mAh/g and 140-150mAh/g respectively) than the longer time heat treated sample [24h.] to show the highest specific capacity values (150-180mAh/g) could be understood. It can be seen from Fig.5b that the samples prepared at 750°C with 24h. under the influence of various cut off voltages such as 4.2, 4.4 and 4.6V exhibited a discharge capacity (Q_{dc20}) of 128.95, 147.15 and 159.48 mAh/g respectively along with good capacity retention even at the 20th cycle. These results are in good agreement with those of the reported discharge capacity values of 120mAh/g and 145mAh/g (4.2V), exhibited by a similar compound by increasing the working cut-off voltage to 4.4V. Thus, it is concluded from charge-discharge studies also that a high calcination temperature of 750°C for 24h. is needed to prepare LiNi_{1/3}Co_{1/3}Mn_{1/3}O₂ cathodes to exhibit the maximum specific capacity of 180mAh/g at a high cut-off voltage of 4.6V.

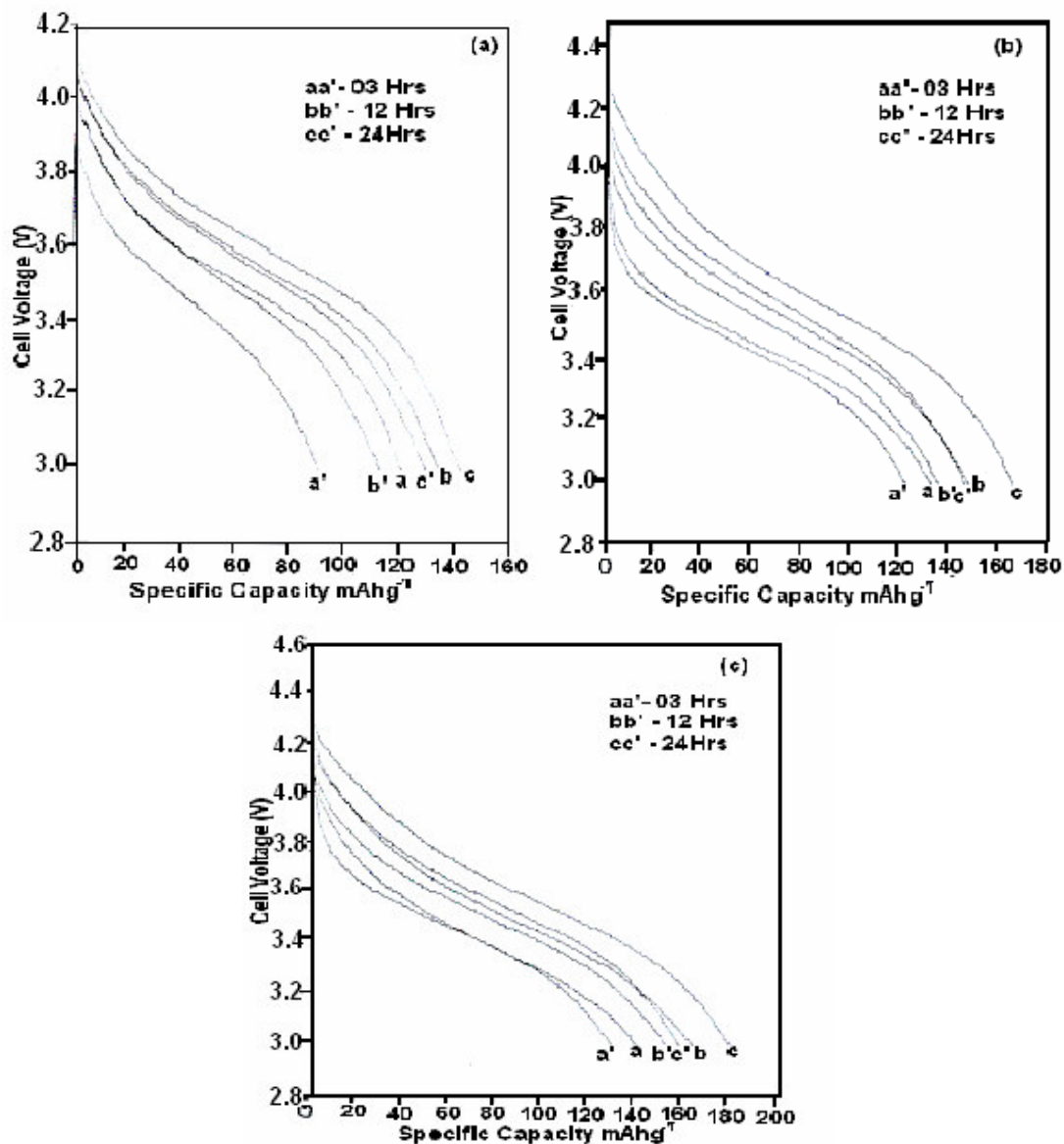


Figure 5. Electrochemical performance of Li/LiNi_{1/3}Co_{1/3}Mn_{1/3}O₂ cells during 1st and 20th cycles as a function of 750°C heat treated cathode prepared at various dwelling times a - Q_{d1} [750°C (3h.)]; a* - Q_{d20} [750°C (3h.)]; b - Q_{d1} [750°C (12h.)]; b* - Q_{d20}[750°C (12h.)]; c - Q_{d1} [750°C (24h.)]; c* - Q_{d20} [750°C (24h.)]

4. CONCLUSIONS

Phase pure LiNi_{1/3}Co_{1/3}Mn_{1/3}O₂ powders with better crystallinity and preferred electrochemical characteristics at high cut-off voltage (4.6V) region has been synthesized by deploying a simple and an easy-to-adopt GAC method. Optimization of reaction conditions such as calcination temperature (750°C) and dwelling time (24h.) has been arrived at, based on the results obtained from both XRD and charge-discharge studies. Impedance analysis favor the charging of LiNi_{1/3}Co_{1/3}Mn_{1/3}O₂ cathodes

up to 4.6V, as the compound becomes a good conductor at 100%SOC condition, to facilitate the process of capacity tapping at high voltage regions. More interestingly, discharge specific capacities in the order of 129mAh/g (4.2V), 147mAh/g (4.4V) and 160mAh/g (4.6V) have been exhibited by $\text{LiNi}_{1/3}\text{Co}_{1/3}\text{Mn}_{1/3}\text{O}_2$ cathode after 20 cycles, thus qualifies itself as one of the high voltage and high capacity cathodes for use in lithium batteries.

References

1. P.G.Bruce, *Chem. Commun.*, (1997) 1817
2. M.M.Thackeray, *Prog. Solid State Chem.* 25 (1997) 1
3. T.Ohzuku, A.Ueda, T.Harai, *Chem.Express*, 7 (1992) 193
4. J.E.Greedan, N.P.Raju, I.J.Davidson, *J.Solid State Chem.*, 128 (1997) 209
5. W.Li, J.C.Currie, *J.Electrochem.Soc.*, 144 (1997) 2773
6. J.M.Kim, H.T.Chung, *J.Power Sources*, 115 (2003) 125
7. Y.I.Chang, B.Haung, H.Wang, D.R.Sadoway, Y.M.Chung, *J.Electrochem.Soc.*, 146 (1999) 3217
8. H.Wang, Y.I.Jang, Y.M.Chiang, *Electrochem.Solid State Lett.* 2 (1999) 490
9. Y.M.Chiang, H.Wang, Y.I.Jang, *Chem.Mater.* 13 (2001) 53
10. J.Cho, B.Park, *Electrochem.Solid State Lett.* 3 (2000) 355
11. J.Cho, Y.J.Kim, B.Park, *Solid State Ionics*, 138 (2001) 221
12. C.Storey, I.Kargina, Y.Grincourt, I.J.Davidson, Y.C.Yoo, D.Y.Seung, *J.Power Sources*, 97-98 (2001) 541
13. Z.P.Guo, *J. Alloys and Compounds* 348 (2003) 231
14. P.G.Bruce, A.R.Armstrong, R.L.Gitzendamer, *J.Mater.Chem.* 9 (1999) 193
15. P.Periasamy, N.Kalaiselvi, *J.Power Sources* (2006) In Press
16. P.Kalyani, N. Kalaiselvi, N.G.Renganathan and M.Raghavan, *Int. J. Ionics*, 9 (2003) 417
17. S.Madhavi, G.V.Subbarao, B.V.R.Chowdari, S.F.Y.Li, *J.Power Sources* 93 (2001) 156
18. C.Delmas, I.Saadome, A.Rougier, *J.Power Sources* 43/44 (1993) 595
19. J.R.Reimers, e.Rossen, C.D.Jones and J.R.Dahn, *Solid State Ionics* 61 (1993) 335
20. G.H.Kim, S.T.Myung, H.S.Kim, Y.K.Sun, *Electrochim.Acta* 51 (2006) 2447
21. S.Madhavi, G.V.Subbarao, B.V.R.Chowdari, S.F.Y.Li, *Solid State Ionics* 152-153 (2002) 199
22. G.T.K.Fey, J.G.Chen, V.Subramanian, T.Osaka, *J.Power Sources* 112 (2002) 384
23. T.Ohzuku, A.Ueda, M.Nagayama, Y.Iwakoshi, H.Komori, *Electrochim.Acta* 38 (1993) 1159
24. Z.Lu, R.A.Donaberger, C.L.Thomas, J.R.Dahn, *J.Electrochem.Soc.*, 149 (2002) A1083
25. R.Koksbang, I.I.Olsen, P.E.Tonder, N.Knudsen, D.Fauteux, *J.Appl. Electrochem.* 21 (1991) 301
26. G.Pistoia, A.Antonin, R.Rosati, D.Zane, *Electrochim.Acta* 141 (1996) 2683
27. G.Montesperelli, P.Nunziante, M.Pasquili, G.Pistoia, *Solid State Ionics* 37 (1990) 149
28. M.Gaberscek, S.Pejovnik, *Electrochim. Acta* 41 (1996) 1137
29. F.Capuano, F.Croce, B.Scrosati, *J.Electrochem.Soc.*, 138(1991) 1918
30. M.D.Levi, K.Gamolsky, D.Aurbach, U.Heider, R.Oesten, *J. Electroanal. Chem.*, 580,2 (2005) 231
31. M.D.Levi, D.Aurbach, *J.Power Sources* 146, 1-2 (2005) 727
32. A.R.Armstrong, A.D.Robertson, R.Gitzendanner, P.G.Bruce, *J. Solid State Chem.*, 145 (1999) 549
33. K. Kubo, S. Arai, S. Yamada and M. Kanda, *J. Power Sources*, Volumes 81-82(1999)59